

MULTITURN INJECTION*

S. Fenster, H. Takeda, and G. Bart[†]
 Argonne National Laboratory
 9700 S. Cass Avenue
 Argonne, IL. 60439

Summary

Several schemes are considered for transverse multi-turn injection into storage rings. Careful attention is paid to geometry and timing of the emittance and acceptance ellipses, while the septum is taken as a line in phase space. The relative shape of input emittance to acceptance is varied, as well as the tune (integer + 1/n) to obtain, before space charge, zero particle loss and minimum dilution $D = \epsilon_A / N \epsilon_i$, where N = number of injected turns, ϵ_A is the machine acceptance, and ϵ_i is the input emittance. Displacement of the IEO by a 4 kick bumper is idealized. The theoretical results for N up to 25 give per-plane dilutions between 1.3 and 2.0. A particle simulation of three schemes to see space charge distortion uses a fast Fourier transform with thin lenses for quadrupoles; wall image is not included. Particle loss on the septum and at the walls is noted and compared. For currents at the conventional space charge limit of the ring, the space charge is a key element in scheme selection.

Phase Space Dilution

Storage rings are used as current multipliers in Heavy Ion Fusion,¹ where multiturn injection implements stacking in the transverse phase planes. The situation is unusual in that particle loss is not permitted for fear of damage to the walls and septum by the ions. The price of zero loss is sizeable dilution of the injector linac emittance beyond the factor N = number of turns. In this note we describe low dilution injection schemes, and present the results of some corresponding particle simulations with space charge.

To each point A around the ring we may associate an azimuth variable θ and two transverse phase space diagrams with axes respectively $x\dot{x}$ and $y\dot{y}$. If we follow a particle and view the local $x\dot{x}$ diagram it will rotate about a point, the instantaneous equilibrium orbit, according to the betatron tune. A scatter plot would show for each turn already injected a distinct roughly uniformly filled ellipse beamlet. The beam extracted after the N turns must be considered as having an emittance equal to the acceptance ϵ_A of the ring, which is $1/\pi$ times the area of the smallest ellipse that contains all the particles for all A . The dilution is defined as

$$D = \epsilon_A / N \epsilon_i$$

where ϵ_i is the emittance of an input beamlet. The septum marking the boundary of the injector is represented by a vertical line in the phase space diagram for the injection location. Particles returning after each passage around the ring must not cross the septum line. This is accomplished by selecting the betatron tune. Thus, before considering space charge, multiturn injection gives rise to the geometric problem of inscribing N equal input ellipses inside a large emittance ellipse with close packing and due respect for the septum. The best schemes have the smallest D (but see below).

Schemes

The equation of an ellipse is taken as

$$\gamma (x-x_0)^2 + \alpha (x-x_0) (x'-x'_0) + \beta (x'-x'_0)^2 = \epsilon$$

and the simplest schemes are those for which emittance and acceptance have equal values of α and β . Then after a coordinate transformation the analysis can be carried out entirely with circles. Improvement can be obtained by varying ϵ_i and β_i so as to minimize D . The geometry of the scheme relates ϵ_i to β_i . Thus, the optimum ϵ_i is determined by differentiation. Table I lists the equal parameter and optimized rotating schemes.

It is assumed that four kickers, two before and two after the septum position, provide fast closed orbit bumping when needed by the schemes.

The injection sequence for $n=4, N=5$ is: start with the IEO at the center of the emittance circle behind the septum. Then, just before the end of the first turn, fast-bump the IEO to the center of the admittance circle. Inject four more turns with tune=integer + 1/4. Finally, just before the end of the fifth turn, fast bump the IEO so that all turns will miss the septum. See Fig. 1A.

Another kind of scheme, called the parallel stack, has the injected ellipses lined up parallel, Fig. 2A. Injection is accomplished by using tune=integer + 1/2 and fast-bumping the IEO in steps equal to one emittance width just before the end of every second turn. The initial IEO position is at the septum in the 1/2 integer case. Optimization leads to formulas for ϵ_0, α_0 and β_0 for arbitrary septum thickness; here we give only the dilutions in Table II.

It may be advantageous to stack in both transverse directions. With single-phase-plane schemes this is accomplished by using two rings in tandem, X-stacking in the first ring and Y-stacking the output of the first ring in the second after a rotation. But, one may also stack in both phase planes using only one ring and a corner septum. Our schemes factorize in X and Y with respect to number of turns and dilution: $N = N_x N_y, D = D_x D_y$. There are several possibilities.

(i) Use a parallel stack in X and some other scheme in Y. The bumping of the septum in X is delayed while N_y turns are injected in Y.

(ii) Use tune=integer + 1/n in X and tune=integer + 1/(n+1) in Y. Then $n(n+1)$ turns are required for complete return so that some cases require no additional bumping.

(iii) Use tune=integer + 1/n in X and tune=integer + 1/n² in Y. See Table III.

Space Charge

Space charge considerations will distort the above picture. To study them we have augmented a purely transverse particle simulation program² and applied it to a storage ring consisting of 20 FODO periods of thin lenses. Stacking is carried out in the X-plane

* Work supported by U. S. Department of Energy.
[†] Truman College, Chicago, IL. 60640

with perfect matching implemented in the Y-plane. Chamber wall image force is not included and the septum has zero thickness. An aperture is established and losses on it and on the septum are logged. Calculations were done with 1024 macro particles for each injected turn. The time step for particle pusher calculations were done with 1024 macro particles for each injected turn. The time step for particle pusher is 1/5 of each lattice period. The initial particle distribution is chosen as K-V for each injected turn. Mesh size, beam size, and time step length were varied by a factor of two with the results unchanged.

Three schemes (a), (b), and (c) were followed. For each scheme two runs were made: one with the interparticle force put equal to zero, and one with the space-charge limited current for the ring.

The cases chosen were N=4 and 5 rotating and N=4 parallel stack. Figures 1 and 2 show the second and third of these. Note the distortion due to space charge, particularly the unexpected hole in Fig. 1c and the elongation in Fig. 2c. Table 4 contains the results of this simulation

Conclusions

This study presents some new multiturn injection schemes and serves as a guide to estimating dilutions. It shows that single-ring two-plane schemes are competitive for large N.

The simulation demonstrated that the space-charge limit current ($\Delta v = 0.25$) is sufficient to distort the beamlets significantly and cause loss and dilution. Some ideas are suggested which have not been carried out. One may enlarge the ring and alter slightly the scheme to maintain 100% efficiency with space charge; the choice of scheme can ultimately be decided this way. One should note that there is an additional subtle aspect of the space charge: there may be no significant enlargement of the smallest circumscribing ellipse, but rather a lumping of the distribution. The ultimate effect of such a nonuniformity in the distribution function can be evaluated only by further downstream considerations.

TABLE I. Dilution of Rotating Schemes

<u>n</u>	<u>N</u>	<u>D</u> (equal param.)	<u>D_{opt}</u>	<u>B_{opt}</u>
2	2	2.00	1.30	0.58
3	3	1.81	1.43	0.54
4	4	2.25	2.00	0.50
	5	1.80	1.60	0.50
	9	2.78		
5	5	3.02		
	6	2.51		
6	6	4.17		

TABLE II. Dilution of Parallel Stack

<u>N</u>	<u>D</u>	<u>N</u>	<u>D</u>
1	1.00	11	1.83
2	1.30	12	1.84
3	1.47	13	1.85
4	1.57	14	1.86
5	1.65	15	1.87
6	1.70	16	1.88
7	1.74	17	1.89
8	1.77	18	1.89
9	1.79	19	1.90
10	1.81	20	1.90

TABLE III. Two-Plane Schemes

Note: a = 1 or 1/2

Any combination of 1 and 1/2 is allowed, except 1/2, 1/2.

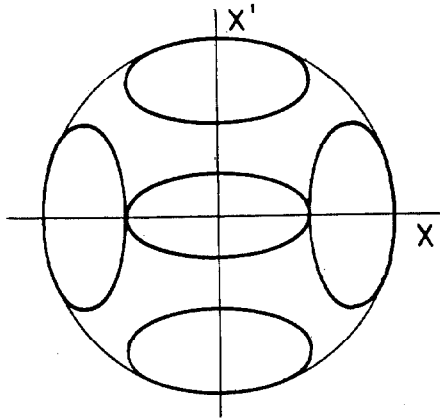
<u>N</u>	<u>D</u>	<u>n_x-1</u>	<u>n_y-1</u>
12	2.25	a	1/3
12	2.31	a	a
12	2.86	1/4	1/3
12	2.94	1/4	1
15	2.29	1/4	1/3
15	2.35	1/4	1
15	2.36	a	1/3
15	2.43	a	a
16	2.46	a	a
16	3.14	1	1/4
16	4.00	1/4	1/16
20	2.51	1/4	1
20	2.59	a	a
20	3.20	1/16	1/4
20	3.30	1	1/4
25	2.56	1/4	1/20
25	2.64	1/4	1
25	2.72	a	a

TABLE IV. Parameters and Results

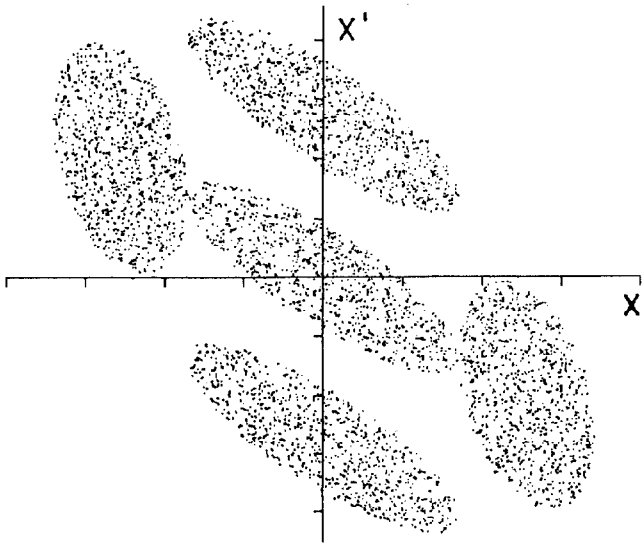
Ring Radius	26.1 m		
Quadrupole Spacings	6.56 m and 1.64 m		
Acceptance X	25.0 mr-cm		
Acceptance Y	3.125 mr-cm		
No. of Macroparticle/Turn	1024		
<u>Scheme</u>	<u>a</u>	<u>b</u>	<u>c</u>
No. Turns	4	5	4
Tune	1/4	1/4	1
Acceptance Ellipse			
α	0.73661	0.73661	0.70711
β	4.67707	4.67707	4.920 m
Beam Ellipse			
α	0.36831	0.36831	0.20676
β	2.33854	2.33854	1.4386 m
ε	3.125	3.125	3.98 mr-cm
Phase Advance/ Period	94.5°	94.5°	90°
Quadrupole Thin Lens Power	0.44776	0.44776	0.43116
Beam Loss Septum	30	203	403
Wall	105	75	0
Total Loss/ Total Beam	3.30%	5.43%	9.84%

References

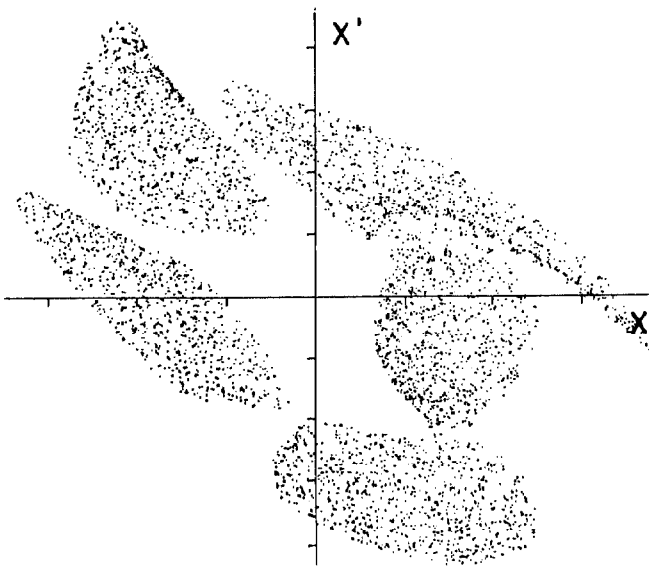
1. Proceedings of the Heavy Ion Fusion Workshop at Argonne National Laboratory, ANL 79-41 (1978)
2. I. Haber, IEEE Transactions on Nuclear Science, NS-26, 3090 (1979).



(A)

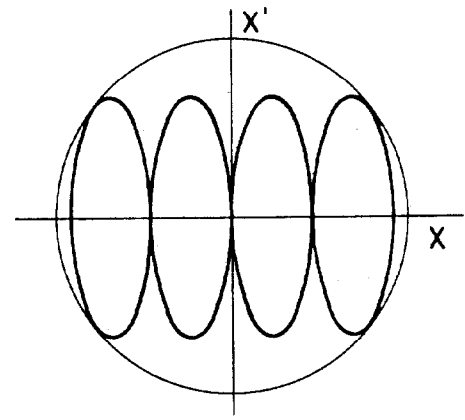


(B)

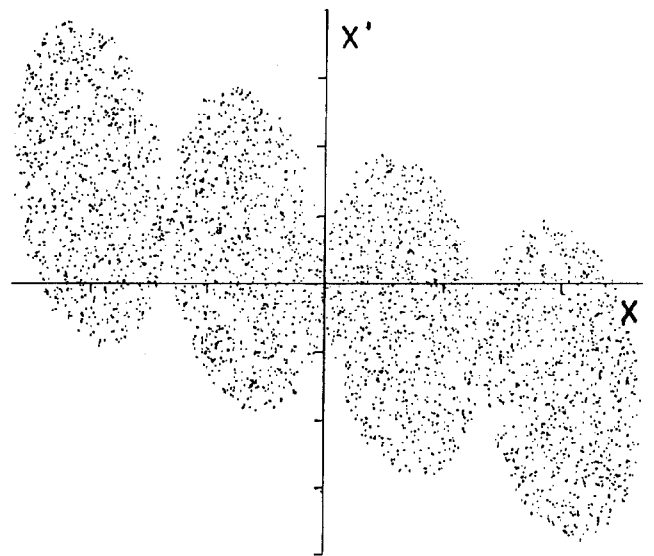


(C)

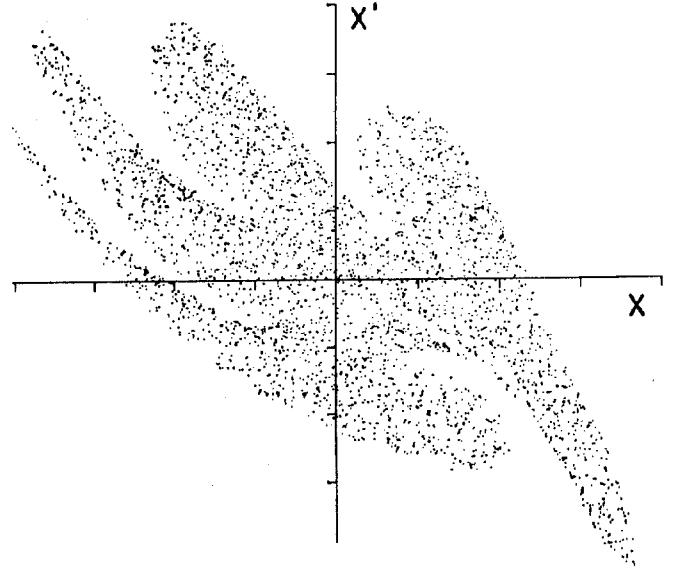
Figure 1 - Scheme (b)



(A)



(B)



(C)

Figure 2 - Scheme (c)

- (A) Phase space configuration of input ellipses.
- (B) Scatter plot with $I = 0$.
- (C) Scatter plot with $I = \text{space charge limit}$.